Quarterly Journal of the Royal Meteorological Society

Q. J. R. Meteorol. Soc. **137**: 224–235, January 2011

Influence of the wind profile on the initiation of convection in mountainous terrain

Martin Hagen,[a]* Joël van Baelen[b] and Evelyne Richard[c]

[a]*Institut für Physik der Atmosphäre, Deutsches Zentrum für Luft- und Raumfahrt, Oberpfaffenhofen, Germany*
[b]*Laboratoire de Météorologie Physique, CNRS and Université Blaise Pascal, Clermont-Ferrand, France*
[c]*Laboratoire d'Aérologie, CNRS and Toulouse University, Toulouse, France*
*Correspondence to: Dr Martin Hagen, DLR Institut für Physik der Atmosphäre, Oberpfaffenhofen, 82234 Wessling, Germany. E-mail: martin.hagen@dlr.de

A number of days with small precipitating convective cells were investigated using weather radars during the COPS (Convective and Orographically-induced Precipitation Study) field campaign in the region of the Vosges and the Rhine Valley in Central Europe. Depending on the weather situation, two distinct mechanisms could be identified for the initiation of convection. On some days, cells were initiated over the ridge of the Vosges, whereas on other days cells were initiated in the lee of the Vosges. The initiation of convection appeared to be concentrated in a few favourable locations. Using the Froude number, it was possible to describe the two distinct mechanisms. When the Froude number was low, the flow was diverted around the Vosges and thermally driven convergence at the ridge initiated convection, whereas when the Froude number was high, the flow passed through mountain gaps and then converged on the lee side with the flow in the Rhine Valley. The convergence on the lee side was enhanced at locations where the outflows through valleys converged. Low Froude numbers were accompanied by weak winds varying with height, whereas high Froude numbers were observed during situations with stronger southwesterly winds increasing with height. Copyright © 2011 Royal Meteorological Society

1. Introduction

Initiation of deep convection requires several ingredients. The surrounding air has to be stratified neutral or unstable, and in addition sufficient moisture is required to enable moist adiabatic ascent of air parcels, but even in an unstable situation the initiation of convection needs some trigger. There might be some area with excess heat sources, or more likely some converging flow which initiates upward motion. This article will concentrate on topographic features which favour the formation of convergence in the sense that convection is frequently released at the same location, a hot spot for deep convection. Banta (1990) gives a summary of several features leading to the initiation of convection in mountainous terrain. In particular he indicates three mechanisms which can trigger clouds: (i) orographic lifting of potential unstable air to the level of free convection; (ii) thermally generated circulation by heating of elevated surfaces or slopes; and (iii) obstacle effects which include gravity waves or convergent flow downstream of a mountain range. A similar but more detailed classification of mechanisms leading to convection in mountainous regions can also be found in Houze (1993, chapter 12).

Quite a number of field campaigns have been devoted to study the orographic impact (or lack of impact) on mesoscale convective clouds and precipitation and to illuminate the effects from different perspectives. The Mesoscale Alpine Programme (MAP, Bougeault *et al.*, 2001;

Volkert *et al.*, 2007) in autumn 1999 had the aim of a better understanding of the precipitation enhancement over high-mountain regions. Similar questions were addressed by the IMPROVE campaign in the northwestern USA (Stoelinga *et al.*, 2003), which considered wintertime stratiform precipitation. CuPIDO (Damiani *et al.*, 2008) was an example of a smaller field campaign dedicated to the specific issue of convection over an isolated mountain. The motivation for the recent campaigns is the desire to improve representation of precipitation in mesoscale numerical models and to improve the forecasting of precipitation.

The aim of this article is to show the influence of the wind field on the initiation of convection in mountainous terrain. We will use radar observations of convective events during the COPS (Convective and Orographically-induced Precipitation Study) campaign. COPS (Wulfmeyer *et al.*, 2008, 2011) was an international field campaign which took place in the Upper Rhine Valley, the Black Forest and the Vosges in Central Europe during summer 2007. The aim of COPS was to study the orographic influence on the initiation and life cycle of convection, with observations from advanced instruments being used to improve the forecast skill of mesoscale numerical models, especially the precipitation forecasts. The region is well known for convective events during summertime, and several studies have shown the effects of orography on convection (e.g. Hannesen, 1998; Gysi, 1998; Dotzek, 2001; Barthlott *et al.*, 2006; Meissner *et al.*, 2007; Behrendt *et al.*, 2011; Corsmeier *et al.*, 2011; Weckwerth *et al.*, 2011).

A large number of convective events where observed during the three-month field campaign (Aoshima *et al.*, 2008). In order to study the triggering of convection in the mountainous region, a number of isolated small convective rain shower events were analysed. The analysis is concentrated on the Vosges and the adjacent Rhine Valley, since the Vosges have a more simple and symmetric shape than the Black Forest, with a steep rise on the western side and a gentle descent on the eastern side.

The paper is organized as follows. Section 2 will describe COPS and the data sources for this study including model simulations. Section 3 will first show results for two consecutive days with quite different convective behaviour, followed by a summary of a number of similar days, and section 4 will summarize the observations and describe the driving forces. Conclusions are in section 5.

2. The COPS field campaign

The COPS field campaign took place during summer 2007 in the area of the Black Forest, Upper Rhine Valley and Vosges in Central Europe (Figure 1). The campaign was embedded in several international projects and aimed to understand convection and precipitation in mountainous terrain. A number of *in situ* and remote-sensing instruments were deployed at five 'supersites'. Three of them were aligned along a transect through Black Forest (Achern, Hornisgrinde and the ARM (atmospheric radiation mission) mobile facility (AMF) at Heselbach). Further to the east, the supersite Deckenpfronn was centred in a network of about 100 weather stations. On the French side of the Rhine Valley, the supersite Meistratzheim was operated with a number of instruments and a nearby X-band radar at Bischenheim. More details on the background for the campaign, its role within other international efforts, the
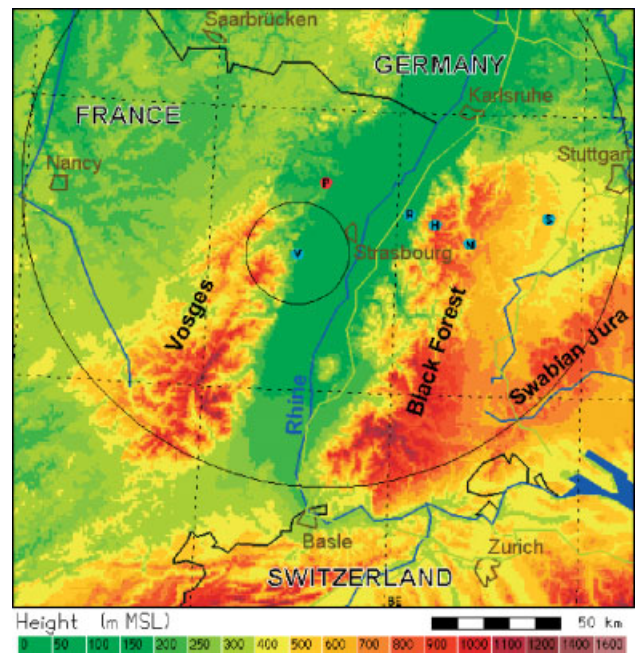

Figure 1. The COPS region in southwestern Germany and northeastern France. Cyan points show locations of supersites: V Bischenberg, R Achern, H Hornisgrinde, M Heselbach, S Deckenpfronn. The range rings are from POLDIRAD (P, red point, 120 km range) and from the X-band radar (V, 20 km range).

strategy of the observations, the variety of the instruments, and some results are given in Wulfmeyer *et al.* (2008, 2011) and Kottmeier *et al.* (2008).

The focus of this study is on the Vosges and the adjacent Rhine Valley. The topographic structure of the Vosges is visible in Figure 1. The southern part reaches up to 1423 m above mean sea level (amsl; Grand Ballon) with deep valleys leading to the ridge. The northern part consists of two 'fingers' orientated southwest to northeast and reaching to 1100 m amsl (Champ du Feu, southern finger) and 1010 m amsl (Rocher de Mutzig, northern finger), respectively. The Bruche Valley is located between the two fingers. The gap, west–east orientated, between the northern and southern part of the Vosges is at about 600 m amsl.

2.1. C-band radar POLDIRAD

Even though the COPS area is well covered by operational Doppler weather radars from Deutscher Wetterdienst, MeteoFrance and MeteoSwiss, there was no polarimetric weather radar in the area. Only the southern part of the COPS region was covered by the French–Swiss polarimetric radar at Montancy in the Jura Mountains. Polarimetric weather radars are established instruments for precipitation research and can provide additional information like hydrometeor classification and improved rain rate estimation. For that reason, the C-band Polarimetric Diversity Doppler Radar (POLDIRAD) of the Deutsches Zentrum für Luft- und Raumfahrt (DLR; Schroth *et al.*, 1988) was deployed for three months in the foothills of the Vosges at Waltenheim-sur-Zorn at 260 m amsl, about 20 km northwest of Strasbourg (Figure 1). Its location was about 100 m above the floor of the Rhine Valley providing an undisturbed overview of the Rhine Valley, the Black Forest and the Vosges. Coincidentally this location was almost exactly in line with the transect of the supersites across the Black Forest.

Volume PPI scans were performed up to 120 km range every 10 min. Also, a RHI scan was performed every 10 min across the Black Forest in line with the supersites at Achern, Hornisgrinde and Heselbach. Since POLDIRAD can not be operated unmanned, observations were normally taken during daytime and in the evening, but for special intensive observation periods (IOPs) the radar was operated through the night to the next day.

2.2. X-band radar at Bischenberg

At the Vosges mountain supersite Bischenberg (Figure 1) the LaMP (Laboratoire de Météorologie Physique, Clermont-Ferrand) high-resolution scanning X-band local area weather radar was installed such that it could monitor the nearby crests of the Vosges to the west as well as the valley plains to the east from the lee of the Vosges up to the Rhine. Although it is neither a Doppler nor a polarized radar, the deployed X-band radar is well suited to document the evolution of precipitation systems due to its high time and space resolution (Van Baelen *et al.*, 2009). For this particular campaign, the radar parameters were set to a range resolution of 60 m up to a maximum range of 20 km, an azimuth resolution of $2°$ and a time resolution of 30 s while the fixed elevation angle was set to $5°$. An attenuation correction was also taken into account by applying a classical Hitschfeld and Bordan (1954) method to the X-band radar reflectivity measurements.

2.3. Numerical simulations using Meso-NH

In addition to the observations, several mesoscale numerical models were used to provide forecasts for the field campaign and to perform studies with different microphysics schemes. For the present study, we used the simulations with the French Meso-NH model (Lafore *et al.*, 1998). The model was run with three nests; the inner nest was centred on the COPS region covering a domain of 400×400 km^2 using a horizontal resolution of 2×2 km^2. In the innermost domain, the convection parametrization was switched off and convection was assumed to be explicitly resolved by a bulk microphysical scheme accounting for cloud droplets, raindrops, ice crystals, snow aggregates, graupel and hail. As a 2 km resolution is still insufficient to entirely resolve convection, in this set-up Meso-NH should be considered as a convection-permitting model rather than a convection-resolving model. The other enabled physical parametrizations were the turbulence, the radiation, and the soil vegetation–atmosphere transfer with land surface parameters provided by 1 km resolution. The initial conditions were obtained from the 0000 UTC analysis from the European Centre for Medium-range Weather Forecasts (ECMWF) and the boundary conditions for the outermost domain were interpolated in time from the 6-hourly ECMWF analyses.

3. Observations of isolated cells

During COPS on several days only small isolated shower or thunderstorm cells developed in the COPS region. Two of these days were 12 and 13 August 2007. On 12 August the cells were initiated along the crest line, whereas on 13 August the cells were initiated in the lee of the Vosges Mountains. In the remainder of this section we will show the observations from different perspectives, and will also summarize the observations from ten other days.

3.1. Mesoscale observations with POLDIRAD

Figure 2 shows two sample plan position indicator (PPI) images of reflectivity factor (linear horizontal polarization) observed by POLDIRAD at $2°$ elevation for the two days. On 12 August, cells developed over the Vosges and then travelled with the mean southwesterly flow into the Rhine Valley while decaying there. On 13 August, the cells developed in the Rhine Valley in the lee of the Vosges and travelled across the Rhine Valley, and some of them were enhanced again at the windward slopes of the Black Forest. According to POLDIRAD's range–height indicator (RHI) measurements, cells reached up to about 7 km amsl on 12 August. On 13 August, some cells reached up to 8 km amsl and reflectivity values were above 60 dBZ with polarimetric radar parameters indicating the presence of hail.

In the course of those two days, a large number of small isolated cells developed over or in the lee of the Vosges. The cells were tracked manually from initiation until decay. Whenever possible, the first visible radar echo with a reflectivity factor larger than 0 dBZ was used to locate the initiation of convection, or to be more precise, the initiation of precipitation. No minimum size was required. Since radar scans were performed only every 10 min, an exact location of the initiation point was not possible. A minimum life time of 30 min was required for a valid selection of the cell. No automatic tracking was possible for cells with low reflectivity factor and size of a few radar range bins only. Also, it was not possible to completely remove clear-air echoes, seen as -10 dBZ values in Figure 2, or ground clutter from Black Forest and Vosges from the radar data. This would limit the use of automatic procedures, therefore a manual tracking was preferred. The location of the cell was identified by the maximum of reflectivity factor, or in case of no pronounced maximum, the centre of the cell area.

Figure 3 shows the cell tracks and location of first radar echo for the two days. The location of the initiation of the cells is markedly different on the two days. In total, 80 (38) cells were tracked on 12 (13) August, with 51 (22) of them initiated over the Vosges or within 10 km of the mountains. On both days, the life time was on the order of 0.5 to 2 h, with some cells being active for even a longer time, mainly on 13 August when some cells did cross the Rhine Valley and were intensified again at the windward slopes of the Black Forest.

3.2. Small-scale observations with the X-band radar

The X-band radar at Bischenberg allows for observations with high temporal and spatial resolution. In Figure 4 the evolution of a cell on 12 August for a 14 min period is shown. This cell decayed later south of POLDIRAD (Figure 2 left, 1440 UTC). These observations show that the cell grew until about 1308, and was then advected with the mean southwesterly wind. Unfortunately the maximum range of 20 km from the radar is not sufficient to observe cells initiated directly at the crest of the Vosges. Figure 5 shows the situation on 13 August when a cell developed in the Rhine Valley just next to the radar, positioned on a small hill close to the exit of the Bruche Valley. It is hypothesized that
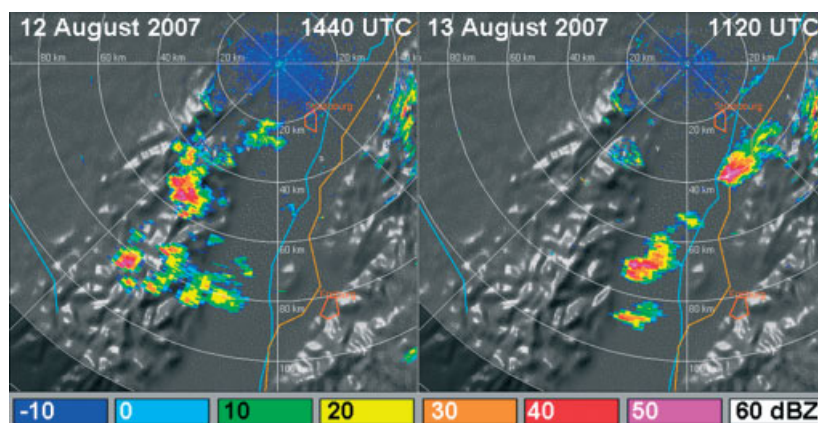
Figure 2. PPI (elevation 2°) of reflectivity factor measured by POLDIRAD at 1440 UTC on 12 August 2007, and at 1120 UTC on 13 August 2007. The range rings are at 20 km intervals. The topography is shown as grey shaded relief.
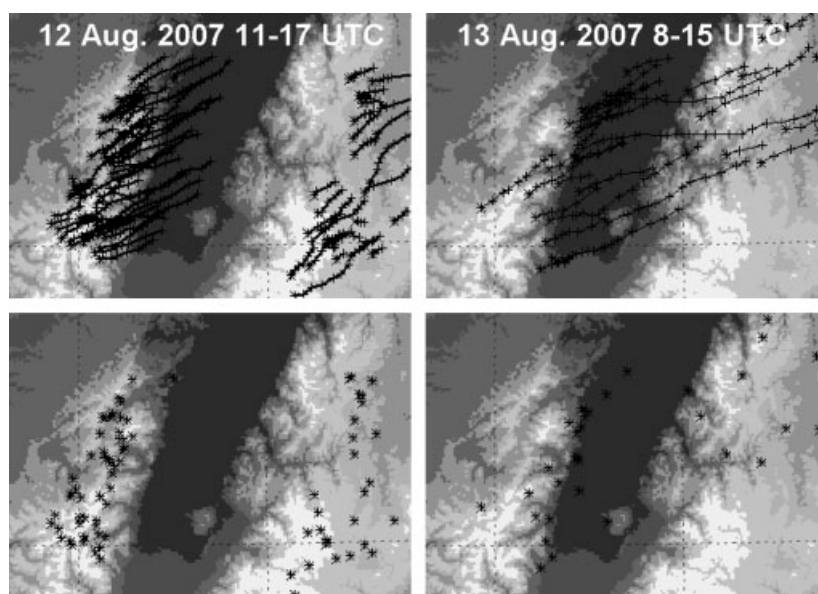

Figure 3. Tracks of cells (top row) and location of first occurrence (bottom row) for 12 and 13 August 2007. The marks along the tracks show location of each cell at 10 min intervals.

the cell is initiated by a convergence of flow coming through the Bruche Valley and southerly flow in the Rhine Valley. An interaction of the flow with the hill is likely. It is possible that the hill has facilitated the initiation of convection at this location.

Similar to Figure 3, cell tracks for a shorter time frame were retrieved from the observations of the X-band radar (Figure 6). Their contours every 10 min are identified as the 30 dBz continuous perimeter around centres of higher reflectivity levels in each radar frame, while the dots indicate the centre of area of the corresponding cell every 30 s. The tracks again show a distinct difference between the two days. On 12 August the cells develop over the mountains of the Vosges and tend to live longer but over a shorter distance, whereas on 13 August the cells develop in the Rhine Valley on the lee side of the Vosges and display a faster displacement with a somewhat shorter lifetime, at least within the field of view of the radar.

3.3. Structure of the atmosphere

Figure 7 shows the temperature profiles and wind profiles from the Nancy radiosonde ascents at 1200 UTC on both

days. Nancy is located about 100 km west of POLDIRAD. The sounding from Nancy was selected to describe the inflow air mass. This station also provides a consistent dataset for the other days discussed in section 3.5. Not all of those days are within IOPs with additional radiosoundings in the Rhine Valley, and thus only the Nancy sounding was available for all days. The stratification is similar on both days, with convective available potential energy (CAPE) quite low ($\sim$125 J kg^{-1}), but in a typical range for Central Europe (e.g. Hagen *et al.*, 1999). CAPE, CIN (convective inhibition) and other parameters (Table I) are discussed later in section 3.5. There is no distinct difference in stratification between the two days. Due to a cold front passage in the late evening of 12 August, the lower troposphere is slightly cooler and dryer on 13 August. Winds below 3000 m amsl are backing on both days, they are weak ($\sim$3 m s^{-1}) on 12 August and have a stronger westerly component (up to 13 m s^{-1}) on 13 August.

To investigate the 2D wind field close to the surface, the Vienna Enhanced Resolution Analysis (VERA; Steinacker *et al.*, 2006) of the surface observations was used. The data basis for the analysis is the joint dataset (Gorgas *et al.*, 2009) which allowed the retrieval of the wind field in the COPS

Table I. Parameters of the 1200 UTC radiosounding ascents at Nancy-Essay for selected days.

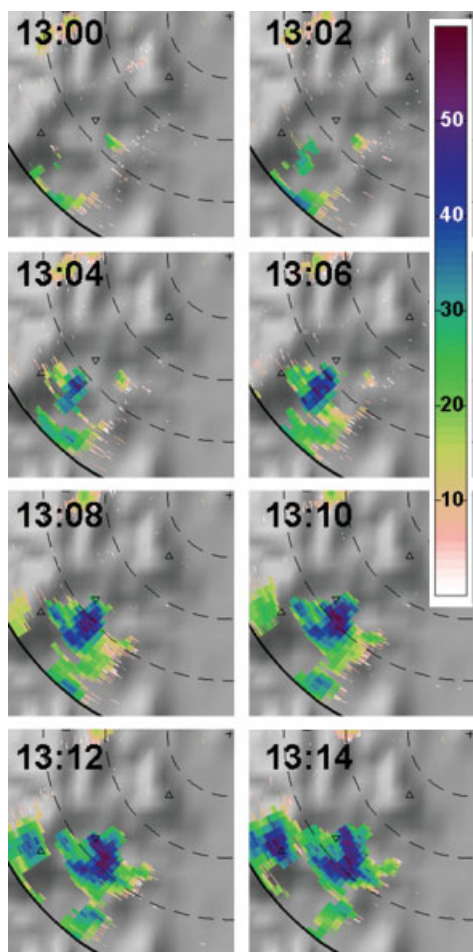| Date	CAPE (J kg^{-1})	CIN (J kg^{-1})	Wind at 700 hPa dir/speed (°/m s^{-1})	Froude number	Brunt–Väisälä frequency 925–700 hPa (s^{-1})	Ridge day (R) Lee day (L)
5 June 2007	339	−32	090/7.0	2.31	0.0074	L
8 June 2007	933	−14	115/5.5	0.64	0.0223	R
9 June 2007	764	−6	210/4.5	0.37	0.0269	R
10 June 2007	1605	−1	225/5.0	0.67	0.0129	R
18 July 2007	82	−16	250/14.5	1.92	0.0119	L
3 Aug 2007	0	0	315/2.5	0.45	0.0189	L
6 Aug 2007	399	−128	235/5.5	0.30	0.0333	L
12 Aug 2007	140	−1	205/3.5	0.33	0.0217	R
13 Aug 2007	102	−2	240/13.5	1.76	0.0146	L
17 Aug 2007	72	−9	235/8.0	1.48	0.0184	L
23 Aug 2007	60	−3	220/7.0	0.94	0.0258	R
24 Aug 2007	524	0	190/7.0	0.95	0.0180	R

Figure 4. X-band radar reflectivity factor (dBZ) observation of a cell development southwest of the radar, 1300–1314 UTC on 12 August 2007. The radar is located in the upper right corner. The range rings are at 5 km intervals. The topography is shown as grey shaded relief.
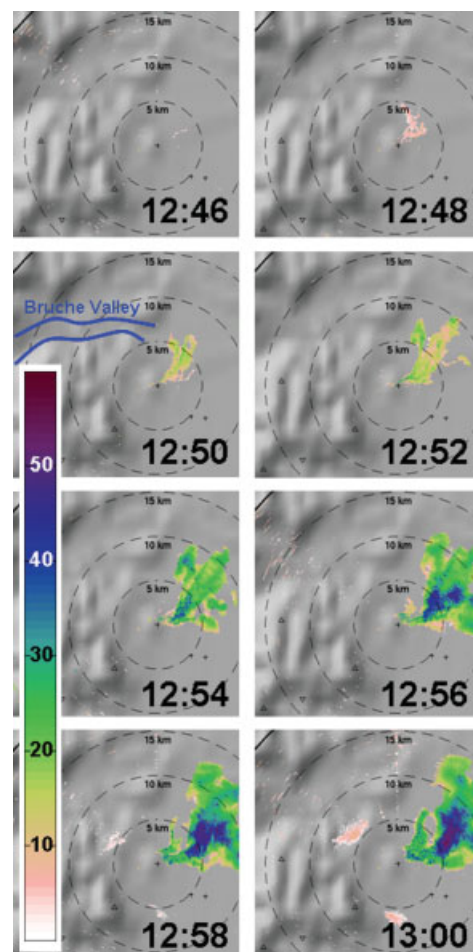

Figure 5. X-band radar reflectivity factor (dBZ) observation of a cell development near the radar, 1246–1300 UTC on 13 August 2007. The radar is located close to the centre. The range rings are at intervals of 5 km. The topography is shown as grey shaded relief.

area at a horizontal resolution of 8 km. In addition, the moisture flux divergence was evaluated. Figure 8 shows the VERA-analysed wind fields leading to the development of convection over and around the Vosges on 12 and 13 August. On the first day, the flow in the lower left corner of the figure indicates weak southwesterly flow which developed parallel

to the Vosges. The inflow from almost all sides towards the Vosges leads to a moisture flux convergence right over the ridge of the Vosges. On 13 August, the flow was more westerly and stronger. Three convergent regions can be located, two of them in the Rhine Valley at the southern and northern ends of the Vosges, and one on the windward side
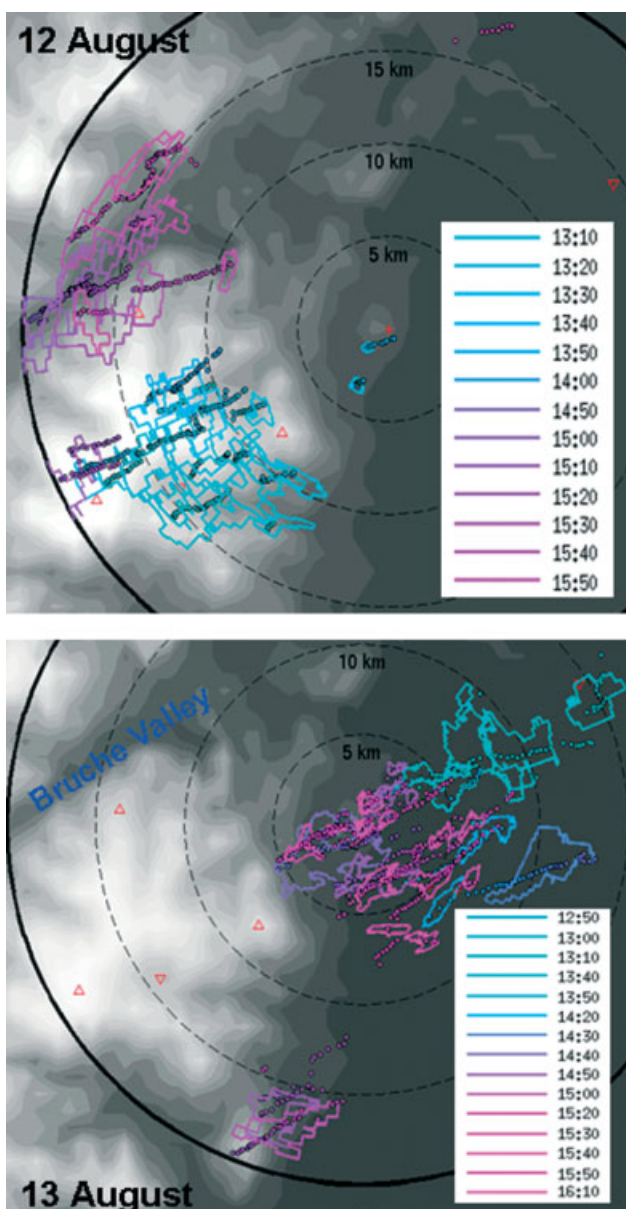
Figure 6. Cell tracks and contour lines at 30 dBZ observed by the X-band radar for 12 August (top, 1310 to 1550 UTC) and 13 August (bottom, 1250 to 1610 UTC). The grey background shows the terrain.

Figure 7. Radiosounding (skew T−log p) at Nancy-Essey at 1200 UTC on 12 August (black lines) and 13 August (red lines). The wind barbs use the standard style (knots). The figure is adapted from the University of Wyoming.

of the Vosges where the southwesterly and northwesterly flows converge. The moisture flux convergence over the Vosges is much weaker than on the day before.

Moisture flux convergence is expected to be a good indicator for future development of convection (e.g. Banacos and Schultz, 2005). However, if its estimation is based solely on surface measurements, it cannot represent all effects leading to convection and, especially in mountainous regions, the analysis is limited by the density and placing of the surface stations (Banacos and Schultz, 2005; Kaufmann, 2006).

Doppler wind measurements with POLDIRAD in clear air (low reflectivity region around the radar in Figure 2) can give information on the wind field, however due to the small area, single-Doppler wind field techniques cannot be applied to retrieve the horizontal wind vector field. It was possible to retrieve wind profiles at the radar site using the VAD technique (Browning and Wexler, 1968). For technical reasons, wind profiles were available only between 1000 and
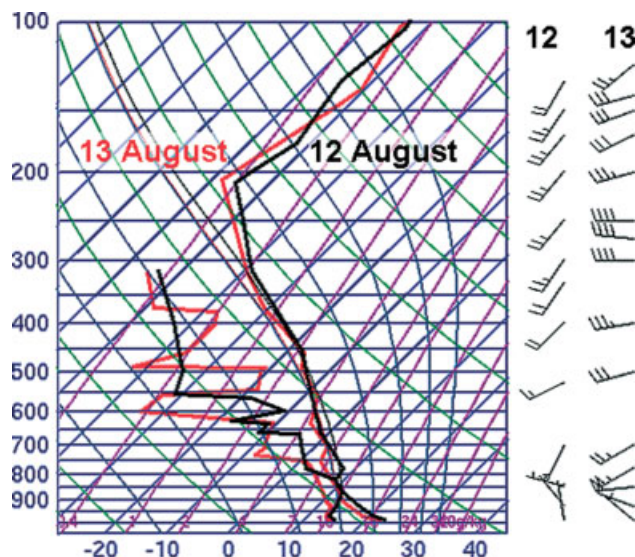
2000 m above ground level (agl) on 12 August, whereas on 13 August clear-air echoes were weaker and did not reach above 1000 m agl. The measurements (not shown) are in agreement with the radiosonde observations and the VERA analysis. Weak northwesterly winds prevailed between 1000 and 2000 m agl on 12 August. On 13 August, a shallow 600 m thick layer with northwesterly winds was observed and strong westerly winds above.

3.4. Numerical simulations using Meso-NH

Since observations could not retrieve the complete 3D wind field, mesoscale simulations will be used to understand the wind field. The Meso-NH simulations have largely been able to reproduce the diverse life cycle of the cells.

Figure 9 shows tracks of precipitation cores (precipitation rate above 2 mm h^{-1}) for the two days, from 1100 to 1700 UTC on 12 August, and from 0800 to 1500 UTC on 13 August (i.e. for the same time periods as in Figure 3). The locations of cell initiation over or near the Vosges on both days are similar to the observed ones (cf. Figure 3). On 13 August, cells were also simulated over the Vosges and on the western slopes. In reality, cells developed over the Vosges about 2 h later, in relation to an approaching trough. In addition, the model initiated cells in the northwest and west of the Vosges on both days. Over the Black Forest, a number of cells were initiated in the simulations whereas only a few cells were observed by the radar (also Bennett et al., 2011).

Considerable discrepancies between observations and simulations occurred in the tracks of the cells. On 12 August the simulated cells stayed with a more southerly flow above the Vosges and did not propagate into the Rhine Valley. On 13 August the tracks of the simulated cells in the Rhine Valley were more easterly than the tracks of the observed ones.

Similar to Figure 8, we show in Figure 10 streamlines with convergence zones at 1000 m amsl from the Meso-NH simulations. Again, as in the observations, on 12 August weak westerly and southwesterly winds prevailed. South of the Vosges, the model shows easterly flow in contrast to the
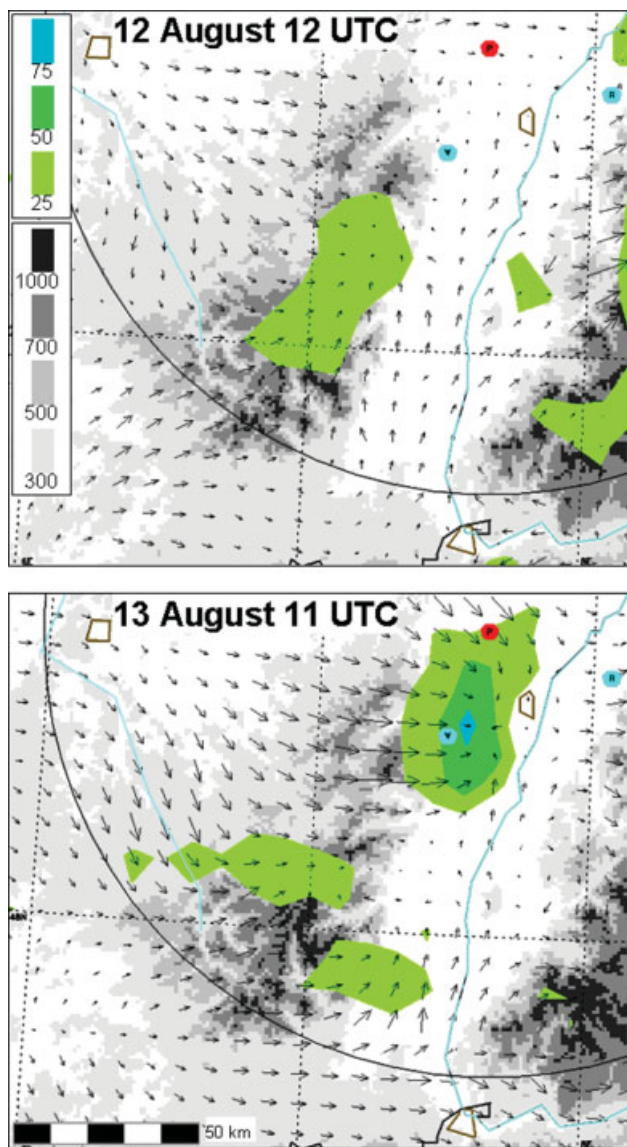
Figure 8. VERA surface analysis of the wind field (5 m s^{-1} corresponds to 10 km on scale) and moisture flux convergence in 10^{-4} g kg^{-1}s^{-1} (green shading). V, P, and R indicate supersites Vosges, POLDIRAD and Achern. Grey shading indicates elevation above 300, 500, 700, and 1000 m amsl.

Figure 9. Tracks of precipitation cores from Meso-NH simulations for 12 (top) and 13 August (bottom). Grey shading indicates terrain above 500, 750, and 1000 m amsl.

observations. Convergence zones along the mountain ridge are caused by valley flow supporting convection driven by elevated heat sources over the mountains. Similar effects were considered by Bennett *et al.* (2011) for the northern Black Forest where convection developed along the eastern flanks (Figure 3) on 12 August.

On 13 August the strong westerly flow is split around the Vosges, strong flow is passing through the gaps between the southern and northern part of the Vosges as well as the northern part of the Bruche Valley. Backing flow can be observed in the southern part of the Rhine Valley. Convergences occur on the rising flanks of the Vosges as well as on the lee side of the Vosges and in the Rhine Valley.

3.5. Observations of further similar events

On a number of other days during the three-month campaign (excluding 14 to 21 June when POLDIRAD was out of order) similar effects were observed. The days are listed together with atmospheric parameters in Table I. The
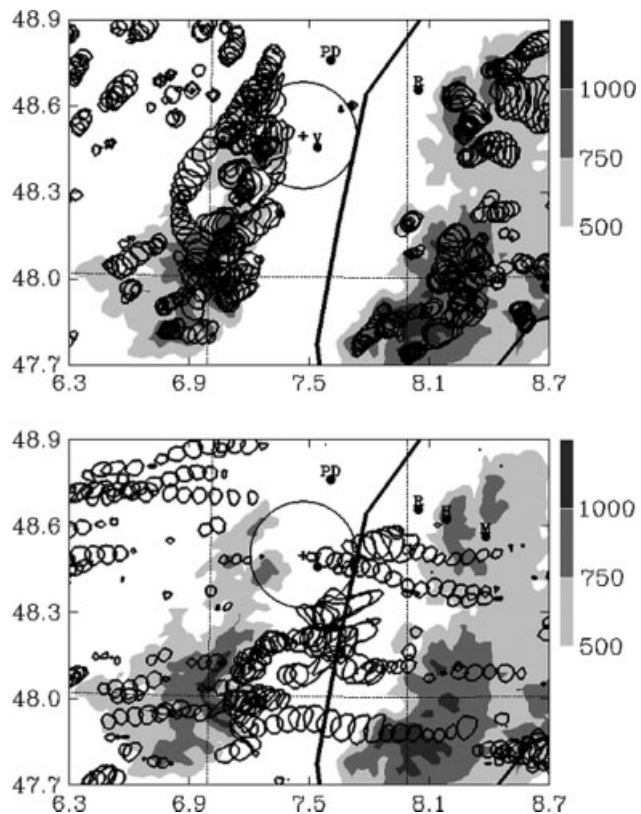
observations with POLDIRAD were analysed as described in section 3.1 and the days were classified according to the majority of the locations where the initiation of the cells was observed. Figure 11 shows the locations of the initiation of cells (including 12 and 13 August) for the two distinct situations. Again, a concentration of points where cells were initiated at the ridge and in the Rhine Valley at the edge of the Vosges can be observed. As in Figure 3, there are locations where the initiation of cells is concentrated on favourable orographic features like the central main mountain ridge or, in the northern Vosges, at ridges along valleys exiting into the Rhine Valley. There is a clear signal in the initiation locations on the eastern side of the Vosges, with numerous initiations on the lee days and almost a complete absence on the ridge days, and vice versa for initiation over the ridge. The initiation of cells west of the Vosges and on the western slopes seems not to be organized; it is likely that convection is released by small-scale disturbances in topography or temperature and humidity. Note that the western slopes are the lee side on 5 June due to easterly winds (Table I). The view of POLDIRAD to the western side of the Vosges is partly obscured by the Vosges and thus it is possible that shallow cells developing further to the west will be visible to the radar at a later stage in their life cycle when they reach greater heights or were advected closer to the radar.

4. Results

The initiation of cells in relation to the Vosges is expected to depend on the interaction between atmospheric flow and orography. As shown by Banta (1990), different mechanisms are possible. The observations (especially for 12 and 13
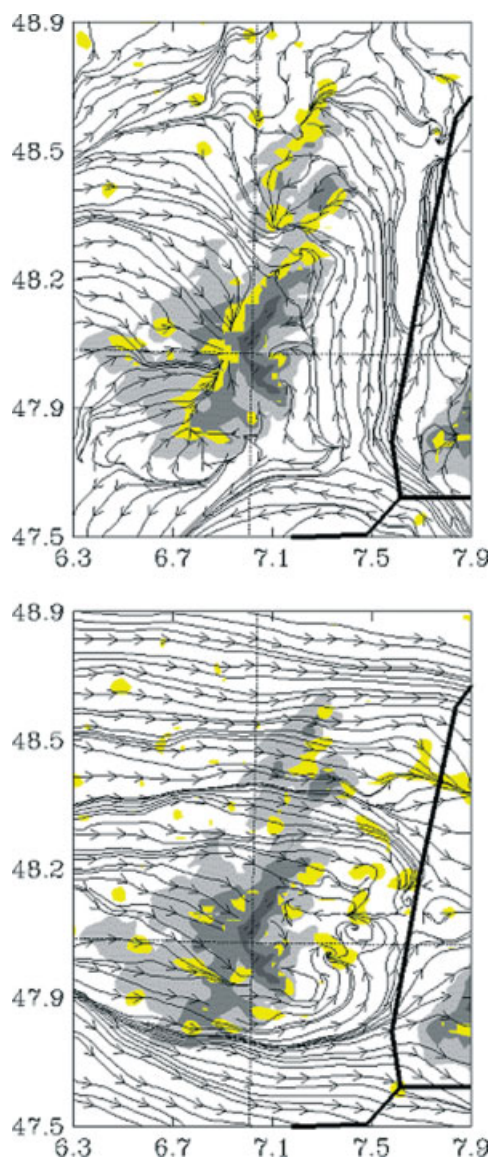
Figure 11. Location of convective initiation for 'ridge' days (top) and 'lee' days (bottom), from POLDIRAD observations. Grey shading indicates elevation above 300, 500, 700, and 1000 m amsl.

Figure 10. Streamlines and wind convergence (yellow: above 0.5×10^{-3} s^{-1}) for 1200 UTC on 12 August (top) and 1100 UTC on 13 August (bottom) from Meso-NH simulations. Grey shading indicates terrain above 500, 750, and 1000 m amsl.

August) showed almost no dependence on the stratification of the atmosphere but a strong dependence on the wind field. Figure 12 shows a wind rose with the wind speed and direction at 925, 850, and 700 hPa from the soundings at Nancy at 1200 UTC on the different days, which represent the upstream flow for most of the selected days. The orientation of the Vosges is indicated by the grey ellipse in Figure 12.

In general on days with initiation over the ridge, weak winds (<5 m s^{-1}) prevail at 925 hPa and wind direction changes with height being perpendicular to the Vosges at 925 hPa and almost parallel to the orientation of the Vosges at 700 hPa. However on 23 August, strong flow parallel to the Vosges is already observed at 925 hPa. For days with initiation in the lee of the Vosges, wind speeds are generally higher at all levels, and wind direction does not change much with height, coming from westsouthwest and so is more perpendicular to the Vosges. On 5 June with easterly winds, initiation of convection was observed at the western slopes of the Vosges. An exception is 3 August with weak winds but development of cells in the lee of the Vosges.
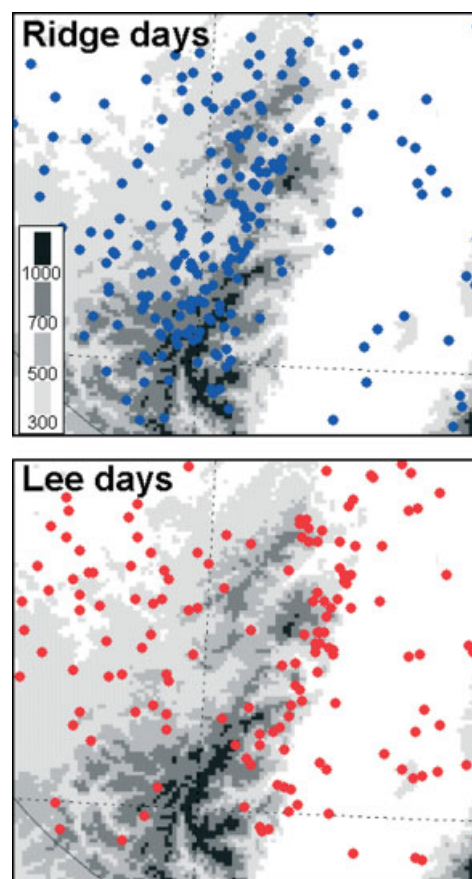
It is quite common to use the Froude number, *Fr,* to study the behaviour of flow over mountains (e.g. Smith, 1979):

$$Fr = \frac{U}{NH}, \qquad (1)$$

where U is a characteristic speed of the flow, H a characteristic height of the mountain and N the Brunt–Väisälä frequency of the flow.

The Brunt–Väisälä frequency is computed using the vertical gradient of the virtual potential temperature of the lower atmosphere between the two standard levels 925 and 700 hPa. For the characteristic speed, the wind speed at 850 hPa is used, and the characteristic height for the Vosges is 800 m. (The peaks reach up to 1100 m amsl in the northern part of the Vosges and 1300 m in the southern part. The region west of the Vosges is at about 250–300 m amsl.) The *Fr* and *N* for the 12 days are listed in Table I. A Froude number below unity indicates that the air flow is stratified stable with a slow speed and the mountain is relatively high. This results in flow around the mountain. For $Fr > 1$, the flow is stronger or the stability is less or the mountain is lower, in this case the flow will be over the mountain. Figure 13 shows the *Fr* for the two distinct situations. It has to be noted that a single sounding cannot be completely representative for a whole region and a time interval of several hours. The standard approach for the use of *Fr* is to analyze air flow which is stably stratified. The described events during COPS are summer events with the potential for deep convection (cf. Table I), thus the flow is nearly neutrally stratified and the estimation of *N* as well
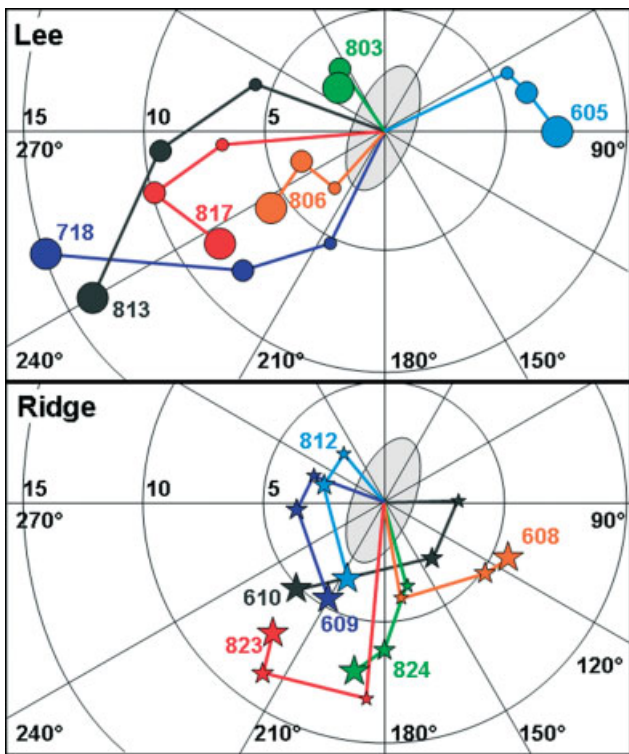
Figure 12. Wind direction and speed (m s^{-1}) from Nancy sounding (1200 UTC) for the 'lee' days (circles, top) and the 'ridge' days (stars, bottom). The size of the symbol indicates the height (small 925 hPa, medium 850 hPa, large 700 hPa). Numbers by the symbols indicate month (first digit) and day (second and third digits). The ellipse shows the orientation of the Vosges.
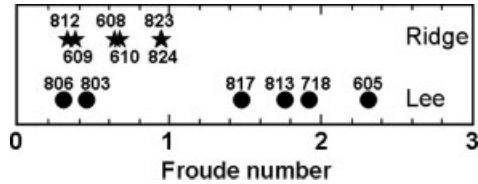

Figure 13. Froude number for 'ridge' days (stars) and 'lee' days (circles). Numbers at the symbols indicate month (first digit) and day (second and third digits).

as Fr is critical and different techniques can be applied (e.g. Reinecke and Durran, 2008).

With the exceptions of 3 and 6 August, the value of Fr determines the mechanisms leading to the development of two different locations for initiation of convection. There is no clear indication why Fr is different for 3 and 6 August than for the other 'lee' days. The unambiguity of the classification on those two days was not different from the other days. One reason is that the wind speed observed at Nancy at the 925 and 850 hPa level is lower than on the other days. The low-level northwesterly flow on 3 August will result in a flow around the northern end of the Vosges. The initiation of convection on 6 August was after the passage of a convergence line in the afternoon, whereas the sounding was in the prefrontal air around noon.

In summary, the mechanisms leading to the two different locations of initiation are sketched in Figure 14. In the situation with a low Fr, the flow is split around the mountain and convection is released through elevated heat islands in the mountains causing convergence at the ridge. With $Fr > 1$, the flow will mainly pass through mountain gaps
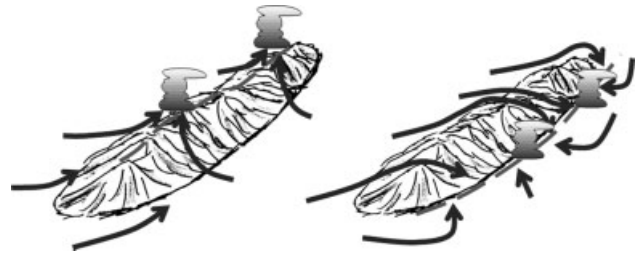

Figure 14. Sketch indicating the mechanisms for 'ridge' initiation and 'lee' initiation of convection at the Vosges. The dashed grey line indicates convergence zones.

and only partly over the Vosges. In conjunction with weak flow or stagnant air in the Rhine Valley and flow around the northern and southern end of the Vosges, this leads to convergence in the Rhine Valley at various locations. The orographic structure of the Vosges and the prevailing wind direction facilitates the flow through the gaps in the mountain ridge and the valleys. Due to the neutral stratification, the situation is different from the classical flow over mountains in stable conditions.

Two further mechanisms can be considered to initiate precipitating convective cells in the lee of the Vosges. One potential mechanism is the triggering of convection by lee waves or rotors. However the flow is not strong enough for the generation of lee waves and the numerical simulations do not show significant downward motion in the lee of the Vosges (Figure 15). However, the absence of initiation between the ridge and the Rhine Valley (Figure 11) might be an indication of subsidence and suppression of convection. The other potential mechanism is the generation of updraughts and clouds at the ridge, but the development of precipitation is delayed by 10 to 30 min and therefore the cells could only be visible to the radar when they were advected later into the Rhine Valley. This hypothesis cannot be confirmed, either from the observations or from the simulations. Figure 5 shows a rapid and almost stationary development of a convective cell in the lee of the Vosges. Meteosat rapid scan visible satellite images with 5 min update rate (not shown) clearly show the stationary development from first clouds to deep convection in the lee with later advection in the Rhine Valley. Numerical simulations (Figure 16) show stationary development of clouds (cyan areas) and precipitation (blue areas) without any advection in the development state, e.g. the two cells developing at the eastern side of the Vosges (indicated by the red arrows in Figure 16). The convergent flow at low levels favours the nearly stationary development from cloud to precipitation. Advection of the cells occurs later when the cells penetrate to heights with higher wind speeds.

5. Discussion and conclusions

A number of days with small precipitating convective cells during the COPS field campaign were investigated using two weather radars in the region of the Vosges and the Rhine Valley. Depending on the weather situation, two distinct mechanisms for the initiation of convection could be identified. On some days, cells were initiated at the ridge of the Vosges, whereas on other days cells were initiated in the lee of the Vosges. These mechanisms were termed by Banta (1990) 'thermal forcing' and 'obstacle effects',
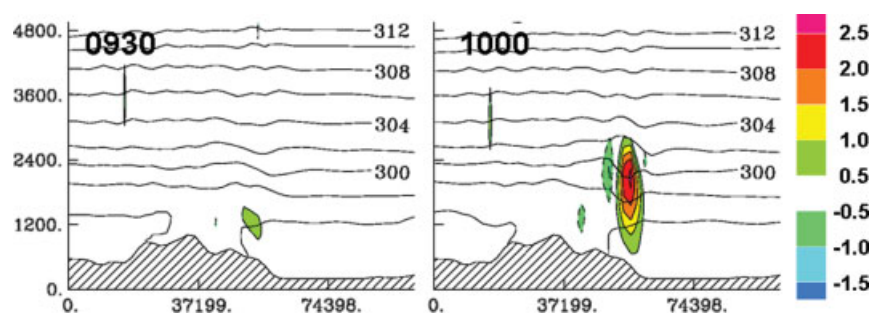
Figure 15. Vertical cross-section along 48°N from numerical simulations for 13 August 2007, at 0930 UTC and at 1000 UTC. The contours are potential temperature (K), and coloured areas indicate vertical air velocity (m s^{-1}).
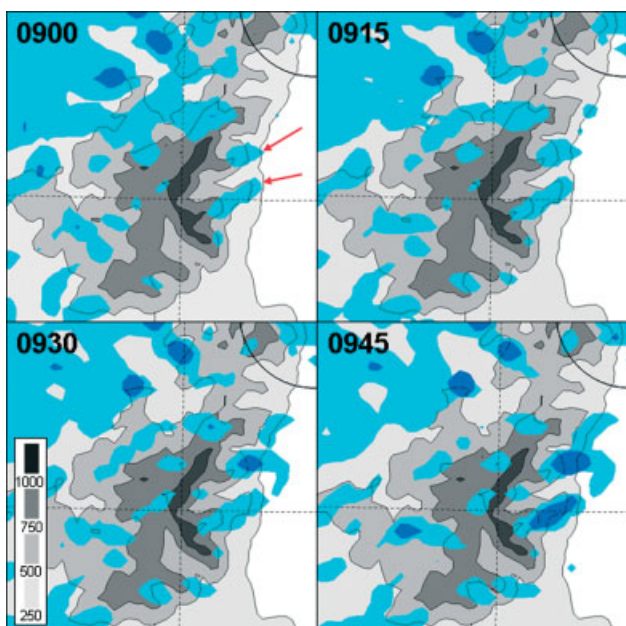

Figure 16. Numerical simulations from 0900 to 0945 UTC on 13 August 2007. Colour shading indicates vertically integrated cloud water (cyan) and rain water (blue) (mm). Grey shading indicates elevation above 250, 500, 750, and 1000 m amsl.

respectively. The lee-side cells initiated frequently in the same area probably as a result of the atmospheric flow interacting with orographic features. We believe the size, shape and orientation of the Vosges to be well suited for this study. Numerical simulations with Meso-NH were used to complete the sparse observations of the wind field around the Vosges. The simulations confirmed the initiation of convection by thermal convergence at the ridge and convergence in the lee, respectively.

The Froude number was used to describe the two distinct mechanisms. When *Fr* was low and winds were weak and varying with height, the flow tended to be diverted around the Vosges, and convection is initialized by thermally driven convergence at the ridge. However, when *Fr* was high and stronger southwesterly winds increasing with height were prevailing, the flow tended to pass through mountain gaps or over the mountains, leading to convergence at the lee side of the mountain with the air in the Rhine Valley. The convergence on the lee side is enhanced at locations where the flow over the mountains is channelled by valleys. Convergence in the lee was also observed at the southern and northern ends of the Vosges where flow around the mountain did interact with the flow in the Rhine Valley.

The observed features are also in agreement with other observations or simulations in the COPS region by Barthlott *et al.* (2006) or Meissner *et al.* (2007). They confirm the initiation of convection at the mountain ridge by a convergence of thermally driven flow from valleys to the ridge. The study of observations and simulations by Thielen and Gadian (1996) in northern England concludes that, for winds not parallel to the ridge, convection is initiated in the lee of the elevated terrain, independent of the inflow direction and the exposure of the slopes to the sun.

Radar observations from the radar at Karlsruhe (Gysi, 1998; Hannesen, 1998) focused on the northern Black Forest and the northern part of the Vosges showed a concentration of severe convection in the region north of the Vosges (the depression of Saverne). This region was found to be a preferred region for the initiation of tornadic storms in southern Germany (Dotzek, 2001). This is attributed to the convergence of flow passing around the Vosges and converging northeast of the Vosges in the Rhine Valley. The typical weather pattern is a strong warm and moist southwesterly flow often combined with cold air advection in the upper troposphere. However, this process is different from the cases described here. Situations like this have been also observed during COPS, but were not considered for the twelve days. Kunz and Puskeiler (2011) describe similar effects at the northeastern edge of the Black Forest and the Swabian Jura. Interestingly, in their study convergence in the lee is observed at low Froude numbers. One other example of convergence in the lee of mountains is the Puget Sound convergence zone (e.g. Chien and Mass, 1997) which is observed also at low *Fr* with flow around the Olympic Mountains in northwestern USA.

Since several studies have observed convergence in the lee of mountains at low Froude numbers, which is in contrast to the observations presented here, it seems necessary to point to the differences and the common facts. Other cases with high *Fr* deal with stable stratification and flow perpendicular to the mountain ridge. In these cases normally no convection is observed in the lee of the mountains since subsiding flow suppresses convection. The key point for the COPS cases seems to be the direction of the flow in combination with the profile of the wind speed; the stratification seems of minor importance. Even though the *Fr* is higher for the COPS cases, the direction of the flow and the orientation of the Vosges, especially the valleys and ridges in the northern Vosges, facilitate flow though gaps and around the mountains and, to a minor extent, flow over the mountain chain itself. The initiation of convection in the lee could be considered as a 'hybrid' situation combining the classical situations of flow around an obstacle and flow over an obstacle.

Even though the mechanisms leading to the two distinct situations for initiation of convection seem quite simple, it is interesting to note that, among several different numerical simulations during COPS (Rotach *et al.*, 2009), a number of models were not able to simulate precipitating convection during 12 and 13 August in the way it was observed. Meso-NH was one of the few successful models. As shown, e.g. by Richard *et al.* (2011), the boundary condition and the initialization of the simulations play an important role for the initiation of precipitating summer convection. This again underlines the importance of understanding the dominating processes in order to improve the skill of numerical simulations of the initiation of precipitation in mountainous terrain.

Acknowledgements

References

Aoshima F, Behrendt A, Bauer H-S, Wulfmeyer V. 2008. Statistics of convection initiation by use of Meteosat rapid scan data during the Convective and Orographically-induced Precipitation Study (COPS). *Meteorol. Z.* **17**: 921–930.

Banacos PC, Schultz DM. 2005. The use of moisture flux convergence in forecasting convective initiation: Historical and operational perspectives. *Weather Forecasting* **20**: 351–366.

Banta RM. 1990. The role of the mountain flow making clouds. In *Atmospheric Processes over Complex Terrain. Meteorol. Monogr.* **23**: Amer. Meteorol. Soc.: Boston. 183–203.

Barthlott C, Corsmeier U, Meissner C, Braun F, Kottmeier C. 2006. The influence of mesoscale circulation systems on triggering convective cells over complex terrain. *Atmos. Res.* **81**: 150–175.

Behrendt A, Pal S, Aoshima F, Bender M, Blyth A, Corsmeier U, Cuesta J, Dick G, Dorninger M, Flamant C, Di Girolamo P, Gorgas T, Huang Y, Kalthoff N, Khodayar S, Mannstein H, Träumner K, Wieser A, Wulfmeyer V. 2011. Observation of convection initiation processes with a suite of state-of-the-art research instruments during COPS IOP 8b. *Q. J. R. Meteorol. Soc.* **137**(S1): 81–100, DOI: 10.1002/qj.758.

Bennett LJ, Blyth AM, Burton RR, Gadian AM, Weckwerth TM, Behrendt A, Di Girolamo P, Dorninger M, Lock S-J, Smith VH, Mobbs SD. 2011. Initiation of convection over the Black Forest mountains during COPS IOP15a. *Q. J. R. Meteorol. Soc.* **137**(S1): 176–189, DOI: 10.1002/qj.760.

Bougeault P, Binder P, Buzzi A, Dirks R, Houze RA, Kuettner J, Smith RB, Steinacker R, Volkert H. 2001. The MAP special observing period. *Bull. Amer. Meteorol. Soc.* **82**: 433–462.

Browning KA, Wexler R. 1968. The determination of kinematic properties of a wind field using Doppler radar. *J. Appl. Meteorol.* **7**: 105–113.

Chien F-C, Mass CF. 1997. Interaction of a warm-season frontal system with the coastal mountains of the western United States. Part II: Evolution of a Puget Sound convergence zone. *Mon. Weather Rev.* **125**: 1730–1752.

Corsmeier U, Kalthoff N, Barthlott C, Behrendt A, Di Girolamo P, Dorninger M, Handwerker J, Kottmeier C, Mahlke H, Mobbs SD,

Norton EG, Wickert J, Wulfmeyer V. 2011. Processes driving deep convection over complex terrain: a multi-scale analysis of observations from COPS IOP 9c. *Q. J. R. Meteorol. Soc.* **137**(S1): 137–155, DOI: 10.1002/qj.754.

Damiani R, Zehnder J, Geerts B, Demko J, Haimov S, Petti J, Poulos GS, Razdan A, Hu J, Leuthold M, French J. 2008. Cumulus photogrammetric, in-situ and Doppler observations: The CuPIDO 2006 experiment. *Bull. Amer. Meteorol. Soc.* **89**: 57–73.

Dotzek N. 2001. Tornadoes in Germany. *Atmos. Res.* **56**: 233–251.

Gorgas T, Dorninger M, Steinacker R. 2009. High resolution analyses based on the D-PHASE and COPS GTS and non-GTS data set. *Ann. Meteorol.* **44**: 94–95.

Gysi H. 1998. Orographic influence on the distribution of accumulated rainfall with different wind directions. *Atmos. Res.* **47–48**: 615–633.

Hagen M, Bartenschlager B, Finke U. 1999. Motion characteristics of thunderstorms in southern Germany. *Meteorol. Appl.* **6**: 227–239.

Hannesen R. 1998. '*Analyse konvektiver Niederschlagssysteme mit einem C-Band Dopplerradar in orographisch gegliedertem Gelände*'. PhD thesis, University of Karlsruhe, Germany.

Hitschfeld W, Bordan J. 1954. Errors inherent in the radar measurement of rainfall at attenuating wavelengths. *J. Atmos. Sci.* **11**: 58–67.

Houze RA. 1993. *Cloud Dynamics.* Academic Press: San Diego and Oxford, UK.

Kaufmann H. 2006. '*Die mesoskalige Analyse der Feuchteflussdivergenz im Alpenraum*'. Diploma thesis, University of Vienna.

Kottmeier C, Kalthoff N, Barthlott C, Corsmeier U, Van Baelen J, Behrendt A, Behrendt R, Blyth A, Coulter R, Crewell S, Di Girolamo P, Dorninger M, Flamant C, Foken T, Hagen M, Hauck C, Höller H, Konow H, Kunz M, Mahlke H, Mobbs S, Richard E, Steinacker R, Weckwerth TM, Wieser A, Wulfmeyer V. 2008. Mechanisms initiating deep convection over complex terrain during COPS. *Meteorol. Z.* **17**: 931–948.

Kunz M, Puskeiler M. 2011. High-resolution assessment of the hail hazard over complex terrain from radar and insurance data. *Meteorol. Z.* **19**: 427–439.

Lafore JP, Stein J, Asencio N, Bougeault P, Ducrocq V, Duron J, Fisher C, Héreil P, Mascart P, Pinty J-P, Redelsperger J-L, Richard E, Vilá-Guerau de Arellano J. 1998. The MESO-NH atmospheric simulation system. Part I: Adiabatic formulation and control simulations. *Ann. Geophys.* **16**: 90–109.

Meissner C, Kalthoff N, Kunz M, Adrian G. 2007. Initiation of shallow convection in the Black Forest mountains. *Atmos. Res.* **86**: 42–60.

Reinecke PA, Durran DR. 2008. Estimating topographic blocking using a Froude number when the static stability is non-uniform. *J. Atmos. Sci.* **65**: 1035–1048.

Richard E, Chaboureau J-P, Flamant C, Champollion C, Hagen M, Schmidt K, Kiemle C, Corsmeier U, Barthlott C, Di Girolamo P. 2011. Forecasting summer convection over the Black Forest: a case-study from the Convective and Orographically-induced Precipitation Study (COPS) experiment. *Q. J. R. Meteorol. Soc.* **137**(S1): 101–117, DOI: 10.1002/qj.710.

Rotach MW, Ambrosetti P, Appenzeller C, Arpagaus M, Fontannaz L, Fundel F, Germann U, Hering A, Liniger MA, Stoll M, Walser A, Ament F, Bauer H-S, Behrendt A, Wulfmeyer V, Bouttier F, Seity Y, Buzzi A, Davolio S, Corazza M, Denhard M, Dorninger M, Gorgas T, Frick J, Hegg C, Zappa M, Keil C, Volkert H, Marsigli C, Montaini A, McTaggart-Cowan R, Mylne K, Ranzi R, Richard E, Rossa A, Santos-Muñoz D, Schär C, Staudinger M, Wang Y, Werhahn J. 2009. MAP D-PHASE: Real-time demonstration of weather forecast quality in the Alpine region. *Bull. Amer. Meteorol. Soc.* **90**: 1321–1336.

Schroth AC, Chandra MS, Meischner PF. 1988. A C-band coherent polarimetric radar for propagation and cloud physics research. *J. Atmos. Oceanic Technol.* **5**: 803–822.

Smith RB. 1979. The influence of mountains on the atmosphere. *Adv. Geophys.* **21**: 87–230.

Steinacker R, Ratheiser M, Bica B, Chimani B, Dorninger M, Gepp W, Lotteraner C, Schneider S, Tschannett S. 2006. A mesoscale data analysis and downscaling method over complex terrain. *Mon. Weather Rev.* **134**: 2758–2771.

Stoelinga MT, Hobbs PV, Mass CF, Locatelli JD, Colle BA, Houze RA Jr, Rangno AL, Bond NA, Smull BF, Rasmussen RM, Thompson G, Colman BR. 2003. Improvement of Microphysical Parameterizations through Observational Verification Experiments (IMPROVE). *Bull. Amer. Meteorol. Soc.* **84**: 1807–1826.

Thielen J, Gadian A. 1996. Influence of different wind directions in relation to topography on the outbreak of convection in northern England. *Ann. Geophys.* **14**: 1078–1087.

Van Baelen J, Tridon F, Pointin Y. 2009. Simultaneous X-band and K-band study of precipitation heterogeneity and associated $Z–R$ relationships. *Atmos. Res.* **94**: 596–605.

Volkert H, Schär C, Smith R. 2007. Editorial: MAP findings. *Q. J. R. Meteorol. Soc.* **133**: 809–810.

Weckwerth TM, Wilson JW, Hagen M, Emerson TJ, Pinto JO, Rife DL, Grebe L. 2011. Radar climatology of the COPS region. *Q. J. R. Meteorol. Soc.* **137**(S1): 31–41, DOI: 10.1002/qj.747.

Wulfmeyer V, Behrendt A, Bauer H-S, Kottmeier C, Corsmeier U, Blyth A, Craig G, Schumann U, Hagen M, Crewell S, Di Girolamo P, Flamant C, Miller M, Montani A, Mobbs S, Richard E, Rotach MW, Arpagaus M, Russchenberg H, Schlüssel P, König M, Gärtner V, Steinacker R, Dorninger M, Turner DD, Weckwerth TM, Hense A, Simmer C. 2008. The Convective and Orographically-induced Precipitation Study: A research and development project of the World Weather Research Program for improving quantitative precipitation forecasting in low-mountain regions. *Bull. Amer. Meteorol. Soc.* **89**: 1477–1486.

Wulfmeyer V, Behrendt A, Kottmeier C, Corsmeier U, Barthlott C, Craig GC, Hagen M, Althausen D, Aoshima F, Arpagaus M, Bauer H-S, Bennett L, Blyth A, Brandau C, Champollion C, Crewell S, Dick G, Di Girolamo P, Dorninger M, Dufournet Y, Eigenmann R, Engelmann R, Flamant C, Foken T, Gorgas T, Grzeschik M, Handwerker J, Hauck C, Höller H, Junkermann W, Kalthoff N, Kiemle C, Klink S, König M, Krauss L, Long CN, Madonna F, Mobbs S, Neininger B, Pal S, Peters G, Pigeon G, Richard E, Rotach MW, Russchenberg H, Schwitalla T, Smith V, Steinacker R, Trentmann J, Turner DD, van Baelen J, Vogt S, Volker H, Weckwerth T, Wernli H, Wieser A, Wirth M. 2011. The Convective and Orographically-induced Precipitation Study (COPS): the scientific strategy, the field phase, and research highlights. *Q. J. R. Meteorol. Soc.* **137**(S1): 3–30, DOI: 10.1002/qj.752.